ECOLOGY LETTERS

Ecology Letters, (2012) **15**: 680–688 doi: 10.1111/j.1461-0248.2012.01785.x

LETTER

Temporal coincidence of environmental stress events modulates predation rates

Sylvain Pincebourde,[1,2*]
Eric Sanford,[3] Jérôme Casas[2] and Brian Helmuth[1]

[1]*University of South Carolina, Environment and Sustainability Program and Department of Biological Sciences, Columbia, SC 29208, USA*

[2]*Institut de Recherche sur la Biologie de l'Insecte, CNRS UMR 7261, Université François Rabelais, 37200 Tours, France*

[3]*Department of Evolution and Ecology, University of California, Davis, California 95616 and Bodega Marine Laboratory, Bodega Bay, CA 94923, USA*

**Correspondence: E-mail: sylvain.pincebourde@univ-tours.fr*

Abstract

Climate warming experiments generally test the ecological effects of constant treatments while neglecting the influence of more realistic patterns of environmental fluctuations. Thus, little is known regarding how the temporal interaction between multiple episodes of thermal stress influences biotic interactions. We measured the sensitivity of predation rate in an intertidal sea star to changing levels of temporal coincidence of underwater and aerial thermal stress events. In laboratory trials, we controlled for intensity, variance and temporal patterning of both underwater and aerial body temperature. Predation rate decreased as underwater and aerial thermal stress episodes became temporally non-coincident, despite a similar intensity and variance among treatments. Experiments under constant conditions were a poor predictor of more complex environmental scenarios because of these strong temporal interactions. Such temporal interactions may be widespread in various ecosystems, suggesting a strong need for empirical studies and models that link environmental complexity, physiology, behaviour and species interactions.

Keywords

Biotic interactions, body temperature, climate change, environmental fluctuations, predation, temporal interactions, thermal stress, variance.

Ecology Letters (2012) **15**: 680–688

INTRODUCTION

Environmental stress is a fundamental factor shaping community structure, biodiversity patterns and levels of ecosystem services (Walther 2010). Stressful conditions alter the physiological ecology of organisms, thereby influencing biotic interactions and initiating effects that may cascade throughout the assemblage (Menge & Sutherland 1987). These functional links have been the focus of increased attention due to the potential impacts of global environmental change on species interactions such as predation and competition. How is climate change influencing the response of organisms to environmental stress? This simple question forces us to realise that some components of environmental stress are still largely ignored. Climate change includes not only a change in mean temperature and its variance (Mearns *et al.* 1997) but also in the frequency and return time of extreme weather events such as heat waves (Easterling *et al.* 2000; Ganguly *et al.* 2009) and cold snaps (Wethey *et al.* 2011). However, the ecological implications of this temporal environmental complexity have been considered only rarely (Benedetti-Cecchi 2003; Denny *et al.* 2009).

There are at least two challenges to identifying the ecological effects of climate-induced thermal stress. First, the impact of stress on the physiological ecology of organisms is often estimated via experiments conducted under constant conditions. Most organisms, however, typically experience fluctuating thermal conditions in their natural habitat. There is concern – and debate – about the pertinence of using thermally constant treatments to estimate the influence of fluctuating temperature on ecological processes (Bannerman *et al.* 2011; Fischer *et al.* 2011; Niehaus *et al.* 2012). Resolving this debate necessitates considering the range within which body temperature fluctuates relative to the (non linear) thermal physiological response curve of organisms (Neuwald & Valenzuela 2011). In addition, the pattern of temporal variation of a factor might set its ecological influence. A temperature change can be described by a change in its mean intensity (average over a given period), its amplitude (variance around the mean) and its temporal variance (return time) (Benedetti-Cecchi 2003; Denny *et al.* 2009). Several studies have quantified the biological effects of changing variance while keeping mean conditions the same (e.g. Brakefield & Kesbeke 1997; Ruel & Ayres 1999; Merakova & Gvozdik 2009; Su *et al.* 2010; Duncan *et al.* 2011). But few have investigated the effect of changing the temporal pattern of variation while both mean and variance are kept at the same levels (e.g. Meats & Kelly 2008). Very little is known, therefore, regarding the interactive effects on biotic interactions of a change in mean, variance and temporal patterns (Benedetti-Cecchi *et al.* 2006; Kearney *et al.* 2012).

Second, organisms are exposed to multiple stresses in their natural habitat. Interactive effects between the mean intensity of several stressors have been documented in various systems (Zvereva & Kozlov 2006; Crain *et al.* 2008; Tylianakis *et al.* 2008). Nevertheless, the level of stress for each environmental variable fluctuates in time and space, and different stresses are correlated with each other to varying degrees (Denny *et al.* 2009, 2011). The temporal pattern of occurrence of a stress relative to others has been shown to affect the diversity and composition of benthic stream assemblages (Garcia Molinos & Donohue 2010) and to cause physiological stress and mortality in intertidal organisms (Denny *et al.* 2009; Williams *et al.* 2011). In these studies, different terms were used to characterise whether or not several stressors occur at the same time, such as 'temporal synchronisation' (Garcia Molinos & Donohue 2010) and 'chance coincidence' or 'co-occurrence' (Denny *et al.* 2009). Here, we use the term 'temporal coincidence' which incorporates the entire range of occurrence probabilities. The influence of temporal coincidence between stressors on biotic interactions remains, however, to be investigated.

In this study, we explored the interactive effects of terrestrial and aquatic body temperature on the feeding rate of the sea star *Pisaster ochraceus*, a keystone intertidal predator (Paine 1966). Intertidal organisms are alternatively exposed to aerial and underwater conditions according to the tide cycle. At low tide, the body temperature of ectotherms differs from ambient air or surface temperature and can fluctuate drastically over short time intervals (minutes), as it is driven by the interaction of multiple environmental factors (Helmuth 1998). In contrast, because of the very high heat conductivity of sea water, the body temperature of organisms that are submerged equilibrates rapidly with water temperature, which fluctuates over a longer time window (Pfister *et al.* 2007). The two temperatures – body temperature when emersed at low tide (BT_e) and when immersed at high tide (BT_i) – might be two distinct stressors, yet it is not known whether or not these two stressors disturb the same physiological pathways (Place *et al.* 2011). Thermal variations of similar amplitude have been shown to have different effects on processes such as thermal tolerance in air and underwater (Jones *et al.* 2009), suggesting that BT_e and BT_i can elicit different physiological responses. BT_e and BT_i were both shown separately to influence predation by the sea star *P. ochraceus* on its prey (Sanford 1999; Pincebourde *et al.* 2008). However, very little is known regarding the interactive effects of concomitant variation in BT_e and BT_i on the strength of this or other species interactions (Yamane & Gilman 2009).

We tested the effects of extreme but non-lethal thermal events on the feeding rate of the sea star *P. ochraceus* by manipulating exposure to elevated BT_e and BT_i. We designed experiments under both constant and fluctuating thermal conditions to identify which parameters among mean, variance, temporal pattern and temporal coincidence cause a shift in feeding rates, and to test whether these shifts observed under fluctuating conditions can be predicted from assays conducted under constant conditions. Based on field body temperature patterns showing that BT_e and BT_i fluctuate independently, we first performed an experiment with factorial combinations of 'constant' low, mid and high BT_i and BT_e. A second experiment tested the effects of increasing complexity of the temporal fluctuations when: (i) only one of the two conditions varied through time, (ii) the two conditions fluctuated in phase through time, and (iii) the two conditions fluctuated out of phase through time. These experiments were designed to separate the effects of mean temperature, variance around the mean and temporal patterning as well as the effect of the level of temporal coincidence between elevated BT_i and BT_e on feeding rates. Overall, our results indicate that the level of temporal coincidence between two stressors strongly modulates feeding rates. This effect could not be predicted from experiments conducted under constant conditions.

MATERIALS AND METHODS

Field temperature recordings

We recorded field body temperatures to characterise realistic temperature treatments for our experiments, and to test whether BT_i and BT_e are correlated with each other. Body temperatures were measured at two different outer coast sites within the Bodega Marine Reserve, Bodega Bay, CA, USA (38°19′ N, 123°04′ W). The first site was sheltered from large waves due to its location inside a semi-protected cove (Horseshoe Cove) while the second (~400 m North from Horseshoe Cove) was fully exposed to breaking waves. Our aim was to record temperature patterns at very different sites and not to quantify the wave splash effect (see Appendix S1 in Supporting Information). To estimate the body temperature of sea stars when exposed at low tide (BT_e), we used biomimetic dataloggers previously shown to mimic accurately the thermal properties of *P. ochraceus* (Pincebourde *et al.* 2008; Szathmary *et al.* 2009). Briefly, the biomimetic datalogger consists of a solid foam disc (Aquazone single-cell foam, Reilly Foam) with a height of 3.7 cm and a diameter of 8.5 cm. Each unit contained a datalogger (i-Button, Maxim, Sunnyvale, CA, USA) that measured temperature to the nearest 0.5 °C every 10 min.

We deployed biomimetic dataloggers at the wave-protected site in 2006 (July and August) and 2007 (March–July) and at the wave-exposed site in only 2007. During each period, up to nine dataloggers per site were fixed on flat rocky surfaces at different intertidal elevations spanning the vertical range of *P. ochraceus* distribution at these field sites (see Appendix S1). Sea water temperature (proxy for BT_i) was retrieved from the same dataloggers during immersion periods, as determined by sorting temperature records based on predicted still tidal elevations.

Experimental design

We sought to quantify the effects of body temperature patterns measured in the field on sea star feeding rate. Laboratory experiments were completed at the Bodega Marine Laboratory in July and August 2007. The setup used for the two experiments enabled us to control both BT_i during high tide, using chilling/heating units (Sea Line SL-1000BH 1HP, Coral Reef Supply, Apple Valley, CA, USA), and BT_e during low tide, using 150 W heatwave lamps (ceramic heat emitter, Rolf C. Hagen, Mansfield, MA, USA) (see Appendix S2). Tidal cycles were simulated in 27 identical aquaria (75 L) by alternating periods with aquaria full and nearly empty of water. Animals were exposed to air daily for 6 h, which corresponds to a realistic emersion period for low to mid-intertidal organisms in this region (Pincebourde *et al.* 2008). Low tide was initiated 50 min later on each subsequent day to mimic the natural tidal rhythm. High tides lasted 18 h and 50 min.

We collected sea stars (*Pisaster ochraceus*) and California mussels (*Mytilus californianus*) in early July 2007 from a rocky intertidal site near the Bodega Marine Reserve. Sea stars were acclimated in aquaria for seven days without food prior to the start of experiments at BT_i ~13 °C and BT_e ~15 °C to place all animals in similar physiological condition (no starvation effect was detected; see Appendix S3). Each aquarium contained four sea stars, as in Pincebourde *et al.* (2008). Mussels (mean shell length ± SD; Experiment 1: 49.0 ± 4.3 mm, n = 2 059; Experiment 2: 49.7 ± 4.7 mm, n = 1 296) were added into the aquaria during the first experimental low tide. Groups of 12 mussels were placed in Petri dishes (diameter 10 cm) five weeks before the experiment to allow them to reattach their byssal threads to the dish. Four Petri dishes were fixed in a similar position in each aquarium. Sea stars were provided with food ad libitum throughout the experiments by replacing the dishes in all aquaria at day 10 and otherwise when needed (no satiation effect was detected; see Appendix S3). Sea star feeding was not altered by potential temperature-induced changes in the physiological state of the mussels (see Appendix S3).

At low tide, we adjusted the position of heat lamps (one per aquarium) to control BT_e which we checked every hour with an infrared imaging camera (ThermaCAM 695, FLIR Systems, Boston, MA, USA). Infrared measurements of body surface temperature accurately predicted internal body temperature to within 1 °C (see Appendix S4). Heat lamps were turned on after 1 h of aerial exposure and adjusted to allow BT_e to increase gradually until the experimental temperature was reached after 3 h of emersion. This temperature was then maintained throughout the last 3 h of aerial exposure. A temperature datalogger (i-Button) was placed in each aquarium to record BT_i and air temperatures every 10 min. Wet body mass (mean ± SD) of sea stars was 205.7 ± 49.1 g and 227.6 ± 45.2 g at the start of Experiments 1 and 2, respectively (n = 108 sea stars for each experiment).

Experiment 1: 'Constant' conditions

Experiment 1 was designed to quantify the interactive effects of mean BT_i and BT_e on the feeding rate of *P. ochraceus*. The BT_i and BT_e levels in each treatment were held constant throughout the experiment. Aquaria were assigned randomly to one of the nine thermal treatments that were maintained for 20 days (20 tide cycles, consisting of one low tide followed by one high tide). Each aquarium was an independent replicate (water was not recirculated among replicates). The nine thermal treatments (n = 3 replicate aquaria per treatment) were defined by crossing each BT_i condition (10.3 ± 1 °C, 13.2 ± 0.4 °C and 16.1 ± 0.5 °C) with each BT_e condition (17.5 ± 1.7 °C, 23.6 ± 1.9 °C and 26.3 ± 1.9 °C). The lethal BT_e limit of *P. ochraceus* is 35 °C (Pincebourde *et al.* 2008).

Experiment 2: Fluctuating conditions

Experiment 2 measured the effects of temporal fluctuations in BT_i and BT_e on the feeding rate of *P. ochraceus*. Independent aquaria were assigned randomly to one of the nine treatments that were maintained for 20 days (20 tide cycles, starting with a low tide). The nine treatments (n = 3 replicate aquaria per treatment) were defined by crossing three BT_i conditions with three BT_e conditions. Treatments were designed to separate the effects of variance around mean temperature, temporal patterning of temperature fluctuations for both environments taken independently, and temporal coincidence level of elevated BT_i and BT_e. The temporal variance (equivalent to the 'waiting or gap time', Cook & Lawless 2007; and 'return time', Denny *et al.* 2009) is used here to describe the temporal pattern of occurrence of thermal events (e.g. the variance in the time interval between successive extreme events; Benedetti-Cecchi *et al.* 2006) – which is not to be confused with frequency (Benedetti-Cecchi 2003). For each variable (BT_i and BT_e), the mean temperature was similar among the 9 treatments (Table 1). Among the three conditions of each variable, one corresponded to constant temperature (named BT_e-Constant and BT_i-Constant; Fig. 1a) to serve as a control for the two other conditions that had a large and equal variance but with a different temporal patterning (Table 1). This control was therefore a replicate of Experiment 1, used subsequently to test the statistical model (see below).

The design of the fluctuating treatments mimicked realistic patterns recorded in the field. The first fluctuating BT_e condition (BT_e-Chronic) followed a step-function, with 10 extreme thermal events occurring successively (long period of an oscillation) (Fig. 1b). The second (BT_e-Acute) was a short-period function with alternation between two days of exposure to high BT_e followed by two days without stress and so on (Fig. 1c). These two designs followed the observation that BT_e can vary markedly between two successive low tides (Pincebourde *et al.* 2008). BT_e-Chronic and BT_e-Acute had the same mean and variance, and only their temporal patterning differed (Table 1). In the two BT_i conditions, we adopted long-period functions with a smooth transition zone of 6 days to mimic the comparatively slow rate of warming and cooling of sea water in the field (White 2007): at the fastest, wind-driven upwelling events can cause BT_i to drop several degrees within a few days, and temperatures warm at a similar rate during upwelling relaxations (Sanford 1999, 2002). The BT_i-Down condition started with an 8-day period of exposure to high BT_i and finished with another 8-day period of exposure to low BT_i (Fig. 1b). The treatment BT_i-Up was the reverse, starting with cold water and finishing with warm water (Fig. 1c). BT_i-Down and BT_i-Up had the same mean and variance, and only their temporal trend differed (Table 1). These treatments were also designed to measure the effect of temporal coincidence between high BT_i and high BT_e (Fig. 2). For example, crossing BT_e-Chronic and BT_i-Down conditions caused the two thermal stress episodes

Table 1 Statistical descriptors of fluctuating immersed (BT_i) and emersed (BT_e) body temperature treatments in Experiment 2. Mean, variance, number (n) of extreme events and temporal patterning were calculated over the 20 days of the experiment. BT_i and BT_e extreme events corresponded to BT_i > 15.5 °C and BT_e > 24 °C. The temporal patterning of the fluctuating temperature treatments was described using two parameters. The period of a sine wave function fitted to the temperature data quantified the duration of a complete theoretical fluctuation cycle. The temporal variance was calculated as the variance in the hourly interval between each subsequent extreme event, assuming that the hypothetical 21st day of the experiment was an extreme event. Compound statistics are given in Appendix S7.

		Basic descriptors			Temporal patterning	
	Treatments	Mean (°C)	Variance around mean	n extreme events	Period (n tide cycles)	Temporal variance
BT_i*	BT_i-Constant	13.6	0.1	0	0	0
	BT_i-Down	13.5	7.2	8	28.0	4767
	BT_i-Up	13.2	7.0	8	26.7	4767
BT_e*	BT_e-Constant	21.6	1.0	0	0	0
	BT_e-Chronic	21.5	15.4	10	23.5	2611
	BT_e-Acute	21.5	16.3	10	4.0	85

*Refer to Figs 1 and 2 for the name of treatments.

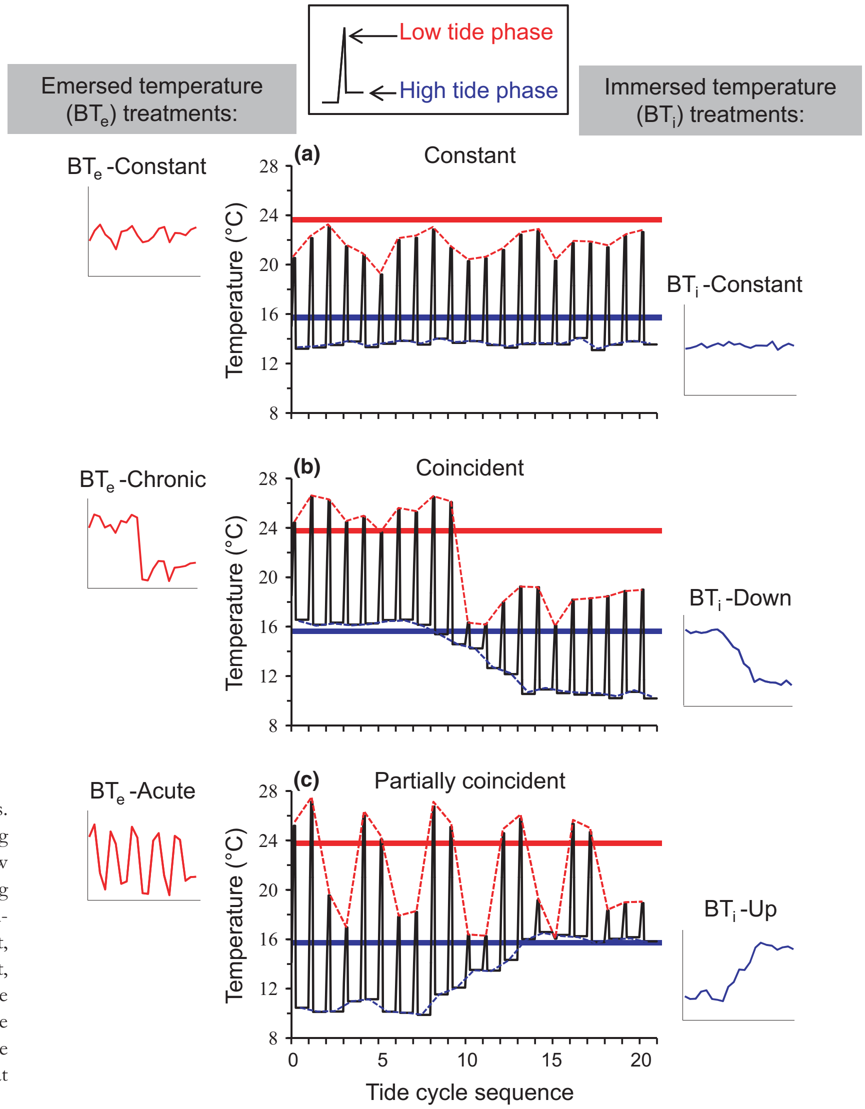

Figure 1 Illustration of the treatments applied in Experiment 2: 'constant' (a), coincident (b) and partially coincident (c) treatments. Each graph indicates the temperature fluctuations as averaged among replicates. Peaks show emersed body temperature (BT_e) during low tides while baselines indicate immersed body temperature (BT_i) during high tides (upper insert). Colour lines depict the schematic representation of BT_e and BT_i conditions shown on the left and on the right, respectively, which were crossed: (a) BT_e-Constant × BT_i-Constant, (b) BT_e-Chronic × BT_i-Down; and (c) BT_e-Acute × BT_i-Up. The three BT_e and the three BT_i conditions are presented. All nine combinations are conceptualised in Fig. 2. Blue and red bands indicate the thermal stress thresholds for BT_i (at ~15.5 °C) and BT_e (at ~24 °C), respectively.

(warm water and warm aerial body) to coincide in time (i.e. on the same day). By contrast, the two stress episodes were non-coincident when crossing BT_e-Chronic and BT_i-Up. Partial temporal coincidence was obtained by crossing the two fluctuating BT_i conditions with BT_e-Acute.

Estimating per capita feeding rate

We collected empty mussel shells in each aquarium during each low tide to estimate the per capita feeding rates. Empty shells were dried, weighed, and their dimensions were measured using callipers. The amount of wet tissue consumed in a single mussel (A, in g) was calculated from the following allometric relationship (linear regression model established from a subset of 60 mussels collected at the same study site; $y = 0.01x - 4.18$; $P < 0.001$, $r^2 = 0.91$; Pincebourde *et al.* 2008)

$$A = [0.01(L \times w) - 4.18] - E$$

where L and w are the shell length and width (mm), respectively, and E is the empty shell mass (g). Per capita feeding rate was calculated by dividing the total amount of mussel tissue consumed by the number of sea stars in each aquarium.

Conceptual approach and statistical modelling

We established a statistical model to test whether feeding rate recorded under constant temperatures (Experiment 1) can predict accurately feeding rates in a fluctuating environment (Experiment 2). This model was designed to predict the per capita feeding rate from BT_i and BT_e during a single tidal cycle. Per capita feeding rates measured in Experiment 1 were first expressed per tide cycle by dividing the total feeding rates by the number of tide cycles. Then, a LOWESS smoothing procedure was used (TableCurve 3D, Systat Software Inc.) to interpolate a complete, high resolution data set from these experimental data points within ranges BT_i 10–17 °C and BT_e 16–28 °C and with a 0.1 °C increment. Then, this interpolated model was used to compute the per capita feeding rate for each tide cycle (one low tide followed by one high tide) from the BT_e-BT_i pairs in Experiment 2, to be compared to measurements in Experiment 2.

Experiment 2 was designed to test for multiple effects. First, we focused on situations when only one factor fluctuated to quantify the effects of increased variance around the mean as well as the effects of varying the temporal patterning of a single factor (Fig. 2). These cases were obtained by crossing the fluctuating conditions of a factor (BT_e-Chronic and BT_e-Acute, or BT_i-Down and BT_i-Up) with the constant condition of the other factor (BT_i-Constant or BT_e-Constant, respectively). Secondly, we focused on the effect of temporal coincidence on feeding rate by crossing all fluctuating conditions (BT_e-Chronic and BT_e-Acute, crossed with BT_i-Down and BT_i-Up). These factorial experiments gave three levels of coincidence: (completely) coincident (all extreme BT_e and BT_i events occurred during the same tidal cycles), partially coincident (half of extreme BT_e events occurred when BT_i was high) and non-coincident (extreme BT_i and BT_e occurred during different periods) (Figs 1 and 2).

Statistical analysis

Field temperature measurements were analysed using Pearson's correlations to assess the level of correlation between BT_i and BT_e. Mixed semidiurnal tides occur at Bodega Bay, corresponding to two high and two low tides of unequal amplitude per day. Here, we included the temperature recordings from the 'low' low tide only, because most loggers remained underwater or splashed by waves during 'high' low tides. Thus, this analysis considered the mean BT_i during a high tide and the maximal BT_e reached at the end of the following low tide. These correlations were made on the complete dataset of BT_i-BT_e pairs of points (i.e. per logger, all tide cycles) to determine which combinations of BT_i-BT_e values were observed in the field.

A two-factor ANOVA was performed to test the effect of BT_i and BT_e on per capita feeding rates in 'constant' conditions (Experiment 1). A Tukey HSD test for multiple comparisons was used for pairwise comparisons. In Experiment 2, the effects of variance, temporal patterning and level of temporal coincidence on per capita feeding rates were tested by running a one-factor ANOVA with a Tukey HSD test for pairwise comparisons. Finally, in Experiment 2, the model

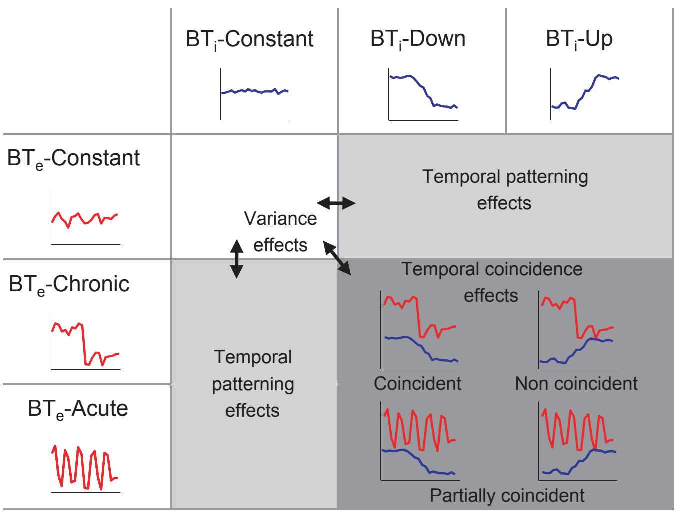

Figure 2 Conceptual approach of Experiment 2. This schematic indicates which comparisons of thermal treatments allow assessment of the influence of variance around the mean (double-headed arrows: comparison of constant vs. one factor-varying treatments), temporal patterning (light grey boxes: comparison among one factor-varying treatments) and level of temporal coincidence (dark grey box: comparison among all two factors-varying treatments) on feeding rate. The different thermal conditions are presented as in Fig. 1.

predictions and the corresponding experimental feeding rates were compared with a paired *t*-test. For all tests, done in SYSTAT 10 (SPSS Inc.), the level of significance was set to 0.05.

RESULTS

Field body temperatures

The daily maximal BT_e ranged from 10 °C to 35 °C with only 10 and 8 days above 30 °C in the wave-protected and wave-exposed sites, respectively (Fig. 3). Microclimatic conditions during low tide, especially ambient air temperature and solar radiation, caused the biomimetic loggers to be warmer than the cold sea water during spring and summer (see Appendix S5). Daily BT_i was weakly correlated with maximal BT_e at low intertidal elevation in the wave-protected site (Pearson's correlation: $P = 0.002$, coefficient = 0.20) (Fig. 3). This correlation did not hold for mid and high intertidal elevations at this site (Pearson's correlation: $P > 0.05$ for all). By contrast, at the wave-exposed site, a weak correlation between BT_i and BT_e was found only at high intertidal elevation (Pearson's correlation: $P < 0.001$, coefficient = 0.24). Overall, a wide range of BT_i-BT_e combinations were observed in the field. Such relative independence justifies the BT_i-BT_e combinations used in Experiments 1 and 2.

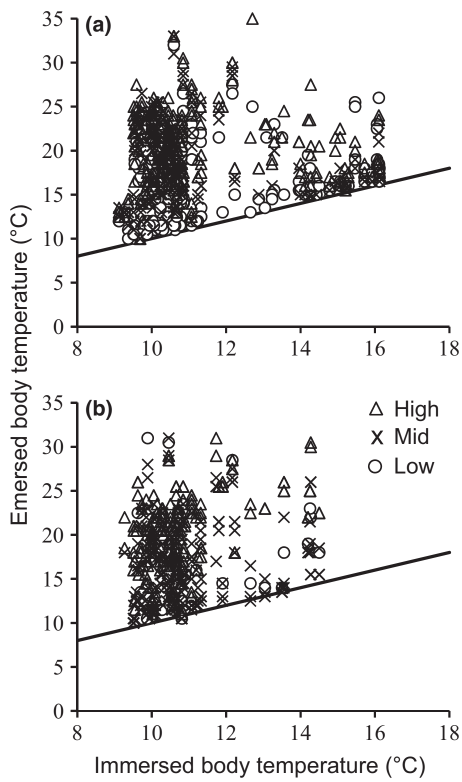

Figure 3 Maximal emersed body temperature (BT_e) during low tide, as measured by biomimetic dataloggers, as function of mean immersed body temperature (BT_i) during the previous high tide in the field for the wave-protected (a) and the wave-exposed (b) sites. Each point represents maximal BT_e and mean BT_i recorded by a datalogger on a given day ('low' low tide, followed by high tide) at a given intertidal elevation (circles: low-intertidal; crosses: mid-intertidal; triangles: high-intertidal zone). A total of 724 and 449 temperatures were recorded from the wave-protected and the wave-exposed sites, respectively. Some biomimetic loggers were lost through dislodgment by waves at the wave-exposed site. Lines indicate equality of temperatures.

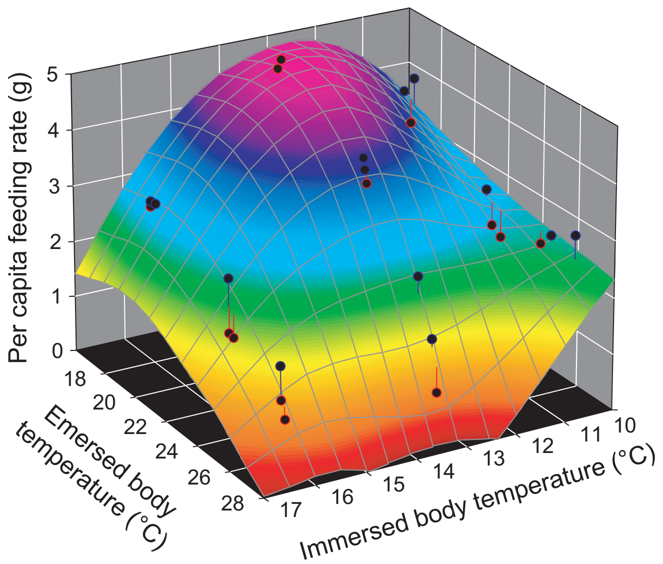

Figure 4 Per capita feeding rate of *Pisaster ochraceus* (expressed per tide cycle) as function of emersed body temperature (BT_e) and immersed body temperature (BT_i) treatments in the Experiment 1. The points represent experimental measurements. The LOWESS smoothing interpolation procedure is shown, the colour indicating the range of feeding rate for easier reading (from red, very low feeding rate, to purple, very high feeding rate). The red and blue lines connecting the datapoints to the interpolated model surface show the negative and positive (respectively) residuals of datapoints to the interpolated model. The grid drawn on the interpolated model surface represents ranges of 0.5 °C for the two variables (BT_i and BT_e).

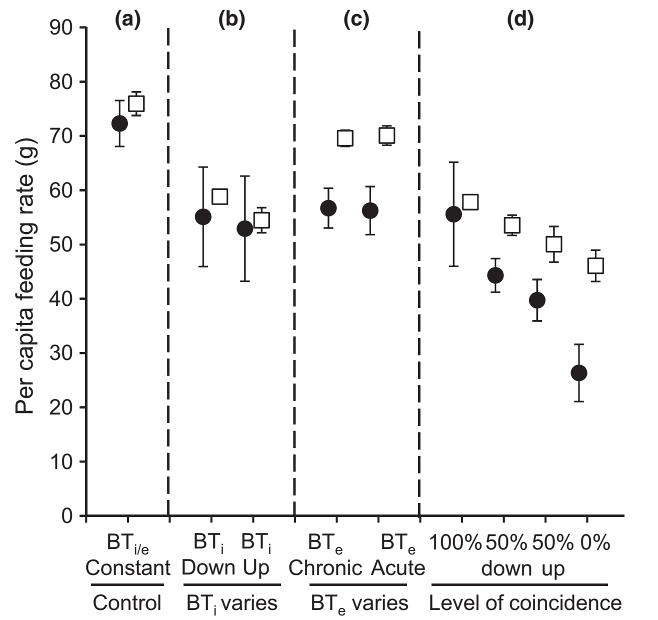

Figure 5 Per capita feeding rate of *Pisaster ochraceus* (total for the 20 days) as function of thermal treatments in Experiment 2. Black points represent experimental means (± SD) and white squares indicate the predictions (mean ± sd) of the interpolated model. (a) 'Constant' condition (control: BT_i-Constant × BT_e-Constant), (b and c) situations with only one of the two variables varying (BT_e-Constant crossed with BT_i-Down and BT_i-Up; BT_i-Constant crossed with BT_e-Chronic and BT_e-Acute), and (d) the two variables fluctuating with different level of temporal coincidence. Complete coincidence (100%) corresponds to BT_e-Chronic × BT_i-Down, partial coincidence to BT_e-Acute × BT_i-Down (50% down) and BT_e-Acute × BT_i-Up (50% up), and non-coincidence (0%) to BT_e-Chronic x BT_i-Up.

Experiment 1: Feeding rate in constant conditions

The mean per capita feeding rate was strongly and interactively influenced by both BT_i and BT_e in 'constant' conditions (ANOVA: $F_{2,18} = 22.8$ and 46.26 for BT_i and BT_e factors respectively, $P < 0.001$ for both, interaction term $BT_i \times BT_e$: $F_{4,18} = 7.37$, $P = 0.001$) (Fig. 4; see Appendix S7). Feeding rate was higher at BT_i 13 °C than at 10 °C and 16 °C under low to moderate BT_e. The BT_i effect, however, was altered by the strong effect of warm BT_e that substantially depressed the feeding rate. Cold water (10 °C) ameliorated the negative impact of high aerial thermal stress compared to warm water (16 °C) (ANOVA, Tukey pairwise comparison: $P = 0.03$) (Fig. 4). The LOWESS smoothing procedure (order: 2; count: 20) indicated that maximum and minimum feeding rates occurred under the following temperature ranges: [BT_i ~13 °C and BT_e ~17 °C] and [BT_i 14–16 °C and BT_e ~27 °C], respectively (Fig. 4) (LOWESS: $SSE = 2.45$; $r^2 = 0.93$; $RMSE = 0.30$ g, corresponding to a prediction error of 6.45%).

Experiment 2: Feeding rate when one factor fluctuates

The two treatments with fluctuating BT_i and constant BT_e had a lower per capita feeding rate compared to the purely 'constant' situation (ANOVA: $F_{2,6} = 5.183$, $P = 0.04$) (Fig. 5a vs. b). Therefore, augmenting the variance of BT_i lowered the feeding rate of *P. ochraceus*. By contrast, the comparison between the two fluctuating treatments (BT_i-Down and BT_i-Up) suggests that the temporal patterning of BT_i had no influence on the feeding rate. In these treatments, experimental feeding rates were predicted well by the statistical model (paired *t*-test: $P > 0.05$, NS).

Fluctuating BT_e also decreased the per capita feeding rate when compared to the 'constant' treatment (ANOVA: $F_{2,6} = 14.76$, $P = 0.005$) (Fig. 5a vs. c). Again, increasing the variance of BT_e led to a depressed feeding rate while the temporal patterning (BT_e-Chronic vs. BT_e-Acute) had no influence. The statistical model, however, did poorly in predicting the experimental results when only BT_e fluctuated (paired *t*-test: $P < 0.001$).

Experiment 2: Feeding rate when two factors vary concomitantly

The per capita feeding rates obtained when both BT_i and BT_e fluctuated were all lower than in the 'constant' scenario. More importantly, the level of temporal coincidence between the stressful ranges of BT_i and BT_e influenced the feeding rate (ANOVA: $F_{4,10} = 27.78$, $P < 0.001$). Surprisingly, the per capita feeding rate decreased substantially as the two stressful episodes became temporally non-coincident (Fig. 5d). Feeding rates were predicted well by the interpolation model when the two stressors were coincident (paired *t*-test: $P = 0.074$, NS), but were not predicted accurately when stressful episodes were partially or non-coincident (paired *t*-test: $P < 0.05$ for all) (Fig. 5d).

DISCUSSION

Environmental fluctuations play a major role in driving ecological processes that can affect the maintenance of biodiversity (Chesson &

Huntly 1997). Yet, the complexity of temporal fluctuations in environmental stress creates major challenges for both modelling and experimental studies of climate change effects (Kingsolver & Watt 1983; Williams *et al.* 2011). Here, we provide evidence for complex interactive effects between two environmental stressors (aquatic and terrestrial body temperatures) on the feeding rate of a keystone predator. Our study is the first to separate experimentally the effects on feeding rate of a change in mean intensity, variance, temporal pattern and temporal coincidence of stress events. Overall, our results highlight the limitations of using constant treatments in thermal physiology and climate change experiments by showing the unexpected direction and amplitude of the temporal coincidence effect on biotic interactions. In their natural habitat, organisms have various strategies to adjust the thermal intensity and variance they experience (e.g. behavioural and physiological thermoregulation; Kearney *et al.* 2009; Pincebourde *et al.* 2009) and possibly also to avoid the (non)coincidence of different stressors.

The comparison of feeding rates obtained in Experiments 1 and 2 addresses the relevance of using constant conditions assays – which are logistically easier to maintain – to predict biological mechanisms under more realistic fluctuating environments. Overall, the temporal non-coincidence of two stressors emerged as the main factor causing a deviation between constant and fluctuating scenarios. The feeding response curve, established from the 'constant' temperature treatments in Experiment 1, accurately predicted feeding rates only under a few of the fluctuating scenarios, when only BT_i varied and when both stresses were temporally coincident. Otherwise, the response curve model overestimated predation rates due to the failure of incorporating the non-coincidence effects as well as the lasting influence of high BT_e (see below). Recently, Fischer *et al.* (2011) noticed that a fluctuating temperature regime increased physiological rates in a butterfly. By contrast, the feeding rate of *P. ochraceus* was lower under the increased thermal variance scenario. Indeed, our thermal treatments fluctuated around the mean up to extreme non-lethal temperatures (BT_i 16 °C and BT_e 27 °C) which have the strongest effect on predation rate due to the non linear relationship between feeding rate and temperature. A similar effect of increased variance on biotic interaction was also found in a modelling study of a prey-predator relationship (White 2007) and on an epidemiological system (Duncan *et al.* 2011). Fluctuations within an optimal temperature range lead to higher physiological rates than fluctuations reaching occasionally sublethal temperatures (Pincebourde *et al.* 2007).

The temporal coincidence level of the two stressors modulated feeding rate. The physiological processes involved in the response to temporal coincidence are not known. Nevertheless, the effect of high BT_e on feeding rate was found to last for at least several days after exposure in *P. ochraceus* (Pincebourde *et al.* 2008). We hypothesise that *P. ochraceus* requires a period free of any thermal stress to either recover from, or compensate for the effects of past exposure. This lasting effect of exposure to high BT_e is supported by findings on gene regulation dynamics associated with protein degradation and rescue following resubmersion in an intertidal mussel species (Place *et al.* 2011). In addition, cold water confers a bioenergetic advantage to sea stars since their food-intake conversion efficiency remains high while feeding rate is low (Sanford 1999, 2002). Therefore, episodes of cold water occurring right after periods of concomitant high aerial and underwater thermal stresses could optimise the capacity of *P. ochraceus* to recover or compensate quickly. By contrast, in the non-coincident treatment, sea stars experienced both the lasting influence of stressful BT_e and underwater stress during the second part of the experimental period. In general, physiological processes associated with recovery may continue for days after thermal stress episodes (e.g. Hsp expression; Bahrndorff *et al.* 2009), and exposure to stress may produce persistent changes (e.g. in the immune system; Karl *et al.* 2011). Therefore, any novel stressful event occurring during these critical periods can have disproportionate consequences. More generally, environmental interactive influences such as those reported here are likely modulated by other factors such as nutrition (Fischer *et al.* 2010) and CO_2 (Zvereva & Kozlov 2006; Gooding *et al.* 2009).

The feeding response to the temporal coincidence of elevated BT_i and BT_e is intriguing. This response occurred even though the overall mean intensity and variance around the mean of BT_i and BT_e were equal across the fluctuating thermal treatments. Predation rate was strongly depressed when the two stressful episodes were temporally non-coincident, i.e. when they followed each other in time without overlapping. By contrast, predation rate was maximised (i.e. predicted by the feeding response curve model) when the two stressful episodes occurred during the same period. This result is consistent with the conclusion reported by Garcia Molinos & Donohue (2010) regarding the impact of temporal coincidence on stream benthic assemblages. They found that the temporal coincidence of distinct disturbances did not necessarily maximise the negative impact of compound perturbations, most likely because biotic recovery was facilitated during the undisturbed periods. Identifying the temporal interaction between multiple stressors and their consequences for ecological systems is highly critical in the context of environmental changes (Tylianakis *et al.* 2008; Harley & Paine 2009; Williams *et al.* 2011). Yet, the role played by the level of temporal coincidence, such as the one we report here, is rarely considered when addressing the mechanisms underlying climate change-induced ecological shifts (Denny *et al.* 2009). Non-coincidence of multiple stressors could lead to 'ecological surprises' (Paine *et al.* 1998) because of the cascading effects from biotic interactions to ecosystem functioning. Therefore, considering the precise timing of stressful events relative to each other is essential when addressing the effects of global change on organismal responses, and ultimately species interactions and distributions. Temporality appears to be a critical parameter in ecological systems including multiple interacting stressors.

In this study, we teased apart complex interactions between the aquatic and terrestrial daily thermal environments. Interestingly, our results can potentially inform our understanding of the response of purely terrestrial organisms that experience diel cycles of thermal fluctuations analogous to that of low tide/high tide cycles. The thermal environments during day and night are quite different. Night-time temperature varies more slowly compared to daytime (body) temperature mainly because of the influence of solar radiation. Higher extreme temperatures are achieved during daytime while lower extremes occur typically during night time. Thus, the environmental statistics of nocturnal and diurnal thermal environment are affected differently by global change (Easterling *et al.* 2000). Activities of organisms are also usually different between these two periods. To date, however, the relative effects of temperature variations during the night and day on the eco-physiology of organisms or community structure remain largely understudied (Alward *et al.* 1999; Meats & Kelly 2008). Conceptual and experimental approaches such as those developed here would likely improve our understanding of the interactive effects of night- and day-time temperatures on ecological processes. More generally, such temporal interactions may be widespread in numerous ecosystems, suggesting a strong need for empirical studies and models that link environmental complexity, physiology, behaviour and species interactions.

ACKNOWLEDGEMENTS

We thank Jackie Sones, the Aquatic Resources Group and the Sanford group at BML for their help with field work and in developing the experimental setup. This research was funded by a grant from the National Aeronautics and Space Administration (NASA: NNG04GE43G) to BH. SP was supported by a Lavoisier fellowship from the French Ministry of foreign affairs (2006–2007), and ES received support from National Science Foundation grant OCE-06-22924. This publication is a contribution of the Bodega Marine Laboratory, University of California Davis.

AUTHORSHIP

SP, ES and BH designed the study. SP performed the research. SP and JC analysed and interpreted the data. SP wrote the manuscript, and all authors contributed substantially to revisions.

REFERENCES

Alward, R.D., Detling, J.K. & Milchunas, D.G. (1999). Grassland vegetation changes and nocturnal global warming. *Nature*, 283, 229–231.

Bahrndorff, S., Mariën, J., Loeschcke, V. & Ellers, J. (2009). Dynamics of heat-induced thermal stress resistance and Hsp70 expression in the springtail, *Orchesella cincta*. *Funct. Ecol.*, 23, 233–239.

Bannerman, J.A., Gillespie, D.R. & Roitberg, B.D. (2011). The impacts of extreme and fluctuating temperatures on trait-mediated indirect aphid–parasitoid interactions. *Ecol. Entomol.*, 36, 490–498.

Benedetti-Cecchi, L. (2003). The importance of the variance around the mean effect size of ecological processes. *Ecology*, 84, 2335–2346.

Benedetti-Cecchi, L., Bertocci, I., Vaselli, S. & Maggi, E. (2006). Temporal variance reverses the impact of high mean intensity of stress in climate change experiments. *Ecology*, 87, 2489–2499.

Brakefield, P.M. & Kesbeke, F. (1997). Genotype-environment interactions for insect growth in constant and fluctuating temperature regimes. *Proc. Royal Soc. Lond. B*, 264, 717–723.

Chesson, P.L. & Huntly, N. (1997). The roles of harsh and fluctuating conditions in the dynamics of ecological communities. *Am. Nat.*, 150, 519–553.

Cook, R.J. & Lawless, J.F. (2007). *The statistical analysis of recurrent events*. Springer Science + Business Media, New York.

Crain, C.M., Kroeker, K. & Halpern, B.S. (2008). Interactive and cumulative effects of multiple human stressors in marine systems. *Ecol. Lett.*, 11, 1304–1315.

Denny, M., Hunt, L., Miller, L. & Harley, C. (2009). On the prediction of extreme ecological events. *Ecol. Monogr.*, 79, 397–421.

Denny, M.W., Dowd, W.W., Bilir, L. & Mach, K.J. (2011). Spreading the risk: small-scale body temperature variation among intertidal organisms and its implications for species persistence. *J. Exp. Mar. Biol. Ecol.*, 400, 175–190.

Duncan, A., Fellous, S. & Kaltz, O. (2011). Temporal variation in temperature determines disease spread and maintenance in *Paramecium* microcosm populations. *Proc. Royal Soc. Lond. B*, 278, 3412–3420.

Easterling, D.R., Evans, J.L., Groisman, P.Y., Karl, T.R., Kunkel, K.E. & Ambenje, P. (2000). Observed variability and trends in extreme climate events: a brief review. *Bull. Am. Meteor. Soc.*, 81, 417–425.

Fischer, K., Dierks, A., Franke, K., Geister, T.L., Liszka, M., Winter, S. *et al.* (2010). Environmental effects on temperature stress resistance in the tropical butterfly *Bicyclus anynana*. *PLoS ONE*, 5, e15284.

Fischer, K., Kölzow, N., Höltje, H. & Karl, I. (2011). Assay conditions in laboratory experiments: is the use of constant rather than fluctuating temperatures justified when investigating temperature-induced plasticity? *Oecologia*, 166, 23–33.

Ganguly, A.R., Steinhaeuser, K., Erickson, D.J. III, Branstetter, M., Parish, E.S., Singh, N. *et al.* (2009). Higher trends but larger uncertainty and geographic variability in 21st century temperature and heat waves. *Proc. Natl. Acad. Sci. USA*, 106, 15555–15559.

Garcia Molinos, J. & Donohue, I. (2010). Interactions among temporal patterns determine the effects of multiple stressors. *Ecol. Appl.*, 20, 1794–1800.

Gooding, R.A., Harley, C.D.G. & Tang, E. (2009). Elevated water temperature and carbon dioxide concentration increase the growth of a keystone echinoderm. *Proc. Natl. Acad. Sci. USA*, 106, 9316–9321.

Harley, C.D.G. & Paine, R.T. (2009). Contingencies and compounded rare perturbations dictate sudden distributional shifts during periods of gradual climate change. *Proc. Natl. Acad. Sci. USA*, 106, 11172–11176.

Helmuth, B. (1998). Interdidal mussel microclimates: predicting the body temperature of a sessile invertebrate. *Ecol. Monogr.*, 68, 51–74.

Jones, S.J., Mieszkowska, N. & Wethey, D.S. (2009). Linking thermal tolerances and biogeography: *Mytilus edulis* (L.) at its southern limit on the east coast of the United States. *Biol. Bull.*, 217, 73–85.

Karl, I., Stoks, R., De Block, M., Janowitz, S. & Fischer, K. (2011). Temperature extremes and butterfly fitness: conflicting evidence from life history and immune function. *Global Change Biol.*, 17, 676–687.

Kearney, M., Shine, R. & Porter, W. (2009). The potential for behavioral thermoregulation to buffer "cold-blooded" animals against climate warming. *Proc. Natl. Acad. Sci. USA*, 106, 3835–3840.

Kearney, M.R., Matzelle, A. & Helmuth, B. (2012). Biomechanics meets the ecological niche: the importance of temporal data resolution. *J. Exp. Biol.* 215, 922–933.

Kingsolver, J.G. & Watt, W.B. (1983). Thermoregulatory strategies in *Colias* butterflies: thermal stress and the limits to adaptation in temporally varying environments. *Am. Nat.*, 121, 32–55.

Mearns, L.O., Rosenzweig, C. & Goldberg, R. (1997). Mean and variance change in climate scenarios: methods, agricultural applications, and measures of uncertainty. *Clim. Change*, 35, 367–396.

Meats, A. & Kelly, G. (2008). Relation of constant, daily fluctuating, and ambient feeding temperature to daily and accumulated consumption of yeast autolysate and sucrose by female Queensland fruit fly. *Entomol. Exp. Appl.*, 129, 87–95.

Menge, B.A. & Sutherland, J.P. (1987). Community regulation: variation in disturbance, competition, and predation in relation to environmental stress and recruitment. *Am. Nat.*, 130, 730–757.

Merakova, E. & Gvozdik, L. (2009). Thermal acclimation of swimming performance in newt larvae: the influence of diel temperature fluctuations during embryogenesis. *Funct. Ecol.*, 23, 989–995.

Neuwald, J. & Valenzuela, N. (2011). The lesser known challenge of climate change: thermal variance and sex-reversal in vertebrates with temperature-dependent sex determination. *PLoS ONE*, 6, e18117.

Niehaus, A.C., Angilletta, M.J.J., Sears, M.W., Franklin, C.E. & Wilson, R.S. (2012). Predicting the physiological performance of ectotherms in fluctuating thermal environments. *J. Exp. Biol.*, 215, 694–701.

Paine, R.T. (1966). Food web complexity and species diversity. *Am. Nat.*, 100, 65–75.

Paine, R.T., Tegner, M.J. & Johnson, E.A. (1998). Compounded perturbations yield ecological surprises. *Ecosystems*, 1, 535–545.

Pfister, C.A., Wootton, J.T. & Neufield, C.J. (2007). Relative roles of coastal and oceanic processes in determining physical and chemical characteristics of an intensively sampled nearshore system. *Limnol. Oceanogr.*, 52, 1767–1775.

Pincebourde, S., Sinoquet, H., Combes, D. & Casas, J. (2007). Regional climate modulates the canopy mosaic of favourable and risky microclimates for insects. *J. Anim. Ecol.*, 76, 424–438.

Pincebourde, S., Sanford, E. & Helmuth, B. (2008). Body temperature during low tide alters the feeding performance of a top intertidal predator. *Limnol. Oceanogr.*, 53, 1562–1573.

Pincebourde, S., Sanford, E. & Helmuth, B. (2009). An intertidal sea star adjusts thermal inertia to avoid extreme body temperatures. *Am. Nat.*, 174, 890–897.

Place, S.P., Menge, B.A. & Hofmann, G.E. (2011). Transcriptome profiles link environmental variation and physiological response of *Mytilus californianus* between Pacific tides. *Funct. Ecol.*, 26, 144–155.

Ruel, J.J. & Ayres, M.P. (1999). Jensen's inequality predicts effects of environmental variation. *Trends Ecol. Evol.*, 14, 361–366.

Sanford, E. (1999). Regulation of keystone predation by small changes in ocean temperature. *Science*, 283, 2095–2097.

Sanford, E. (2002). The feeding, growth, and energetics of two rocky intertidal predators (*Pisaster ochraceus* and *Nucella canaliculata*) under water temperatures simulating episodic upwelling. *J. Exp. Mar. Biol. Ecol.*, 273, 199–218.

Su, Y., Ma, S. & Feng, C. (2010). Effects of salinity fluctuation on the growth and energy budget of juvenile *Litopenaeus vannamei* at different temperatures. *J. Crust. Biol.*, 30, 430–434.

Szathmary, P., Helmuth, B. & Wethey, D.S. (2009). Climate change in the rocky intertidal zone: predicting and measuring the body temperature of a keystone predator. *Mar. Ecol. Prog. Ser.*, 374, 43–56.

Tylianakis, J.M., Didham, R.K., Bascompte, J. & Wardle, D.A. (2008). Global change and species interactions in terrestrial ecosystems. *Ecol. Lett.*, 11, 1351–1363.

Walther, G.R. (2010). Community and ecosystem responses to recent climate change. *Philos. Trans. R. Soc. B*, 365, 2019–2024.

Wethey, D.S., Woodin, S.A., Hilbish, T.J., Jones, S.J., Lima, F.P. & Brannock, P.M. (2011). Responses of intertidal populations to climate: effects of extreme events versus long term change. *J. Exp. Mar. Biol. Ecol.*, 400, 132–144.

White, D. (2007). Variance in water temperature as a factor in the modelling of starfish and mussel population density and diversity. In: *Advances in Artificial Life, 9th European Conference, ECAL 2007, Lisbon, Portugal, September 10–14, 2007. Proceedings* (eds Almeida e Costa, F., Rocha, L., Costa, E., Harvey, I. & Coutinho, A.). Springer Berlin, Heidelberg, pp. 153–162.

Williams, G.A., DePirro, M., Cartwright, S., Khangura, K., Ng, W.-C., Leung, P.T.Y. *et al.* (2011). Come rain or shine: the combined effects of physical stresses on physiological and protein-level responses of an intertidal limpet in the monsoonal tropics. *Funct. Ecol.*, 25, 101–110.

Yamane, L. & Gilman, S.E. (2009). Opposite responses by an intertidal predator to increasing aquatic and aerial temperatures. *Mar. Ecol. Prog. Ser.*, 393, 27–36.

Zvereva, E.L. & Kozlov, M.V. (2006). Consequences of simultaneous elevation of carbon dioxide and temperature for plant–herbivore interactions: a metaanalysis. *Global Change Biol.*, 12, 27–41.

SUPPORTING INFORMATION

Additional Supporting Information may be downloaded via the online version of this article at Wiley Online Library (www.ecologyletters.com).

As a service to our authors and readers, this journal provides supporting information supplied by the authors. Such materials are peer-reviewed and may be re-organised for online delivery, but are not copy-edited or typeset. Technical support issues arising from supporting information (other than missing files) should be addressed to the authors.

Editor, Tim Wootton
Manuscript received 6 January 2012
First decision made 2 February 2012
Second decision made 17 March 2012
Manuscript accepted 21 March 2012

Appendix S1. Intertidal location of the biomimetic dataloggers

Biomimetic dataloggers (Pincebourde *et al.* 2008) were deployed in the field at different intertidal elevations. To measure representative body temperatures of *Pisaster ochraceus*, we first identified the vertical range of sea star populations at the two study sites. The position relative to mean lower low water (MLLW) of every individual was measured using a surveyor's equipment (laser level). We surveyed a total of 554, 617 and 926 individuals at the wave-protected site in 2006 (8 days) and 2007 (12 days), and the wave-exposed site in 2007 (9 days), respectively. The vertical range of *P. ochraceus* distribution at the wave-exposed site was higher than that at the wave-protected site presumably because of the differential effects of wave splash (Fig. S1). We also measured the upper and lower bounds of the mussel bed at these two sites to establish a comparison between the wave-protected and the wave-exposed areas (Fig. S1). We used the same laser level to measure the upper and the lower limits of the bed every meter along a 25 m horizontal transect. At the wave-exposed field site, it was extremely difficult to deploy dataloggers down to the lower boundary of the mussel bed due to high wave exposure and infrequent emersion. However, the dataloggers at the lowest intertidal elevation that we were able to access are most likely representative of the body temperatures experienced lower in the intertidal zone because of the role of wave splash. The dataloggers considered to be in the low intertidal zone at the wave-exposed site recorded very similar temperatures compared to the low intertidal dataloggers at the wave-protected site. However, we did not have replicate sites within each wave exposure, so we are not able to test explicitly how wave splash might have influenced the body temperature patterns that we recorded. In our study, the effect of wave splash on body temperatures cannot be distinguished from other processes generating thermal heterogeneity like substrate orientation and slope or nature of the substrate.

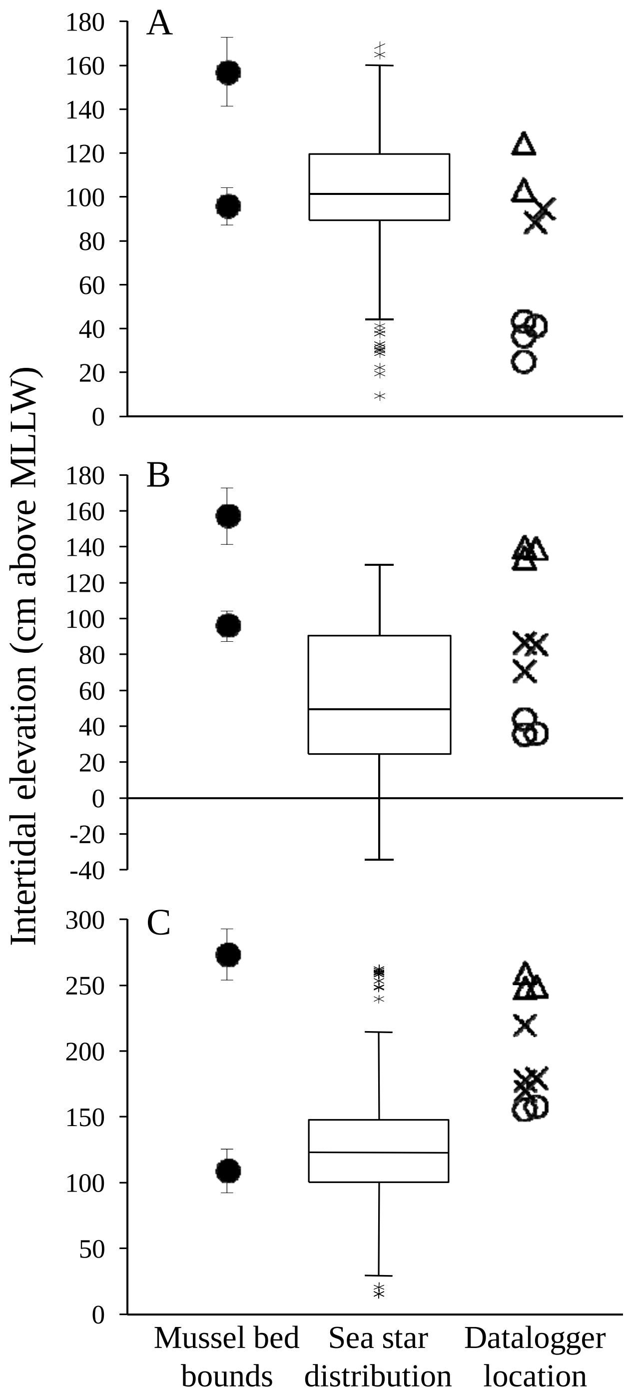

Figure S1. Upper and lower bounds (mean ± SD) of the mussel bed, *Pisaster ochraceus* distribution along the vertical intertidal elevation gradient, and intertidal elevation of the biomimetic dataloggers (circles: low intertidal; crosses; mid intertidal; triangles: high intertidal zone) at the wave-protected site in 2006 (A) and 2007 (B), and the wave-exposed site in 2007(C). The distribution of *P. ochraceus* is shown as box plots: the box corresponds to the 50% central values (the horizontal line in the middle is the median), the whiskers represent the data within inner fences (1.5 times the box height above the box) and the asterisks are the data falling outside of the fences.

REFERENCES

Pincebourde, S., Sanford, E. & Helmuth, B. (2008). Body temperature during low tide alters the feeding performance of a top intertidal predator. *Limnol. Oceanogr.*, 53, 1562-1573.

Appendix S2. Experimental design

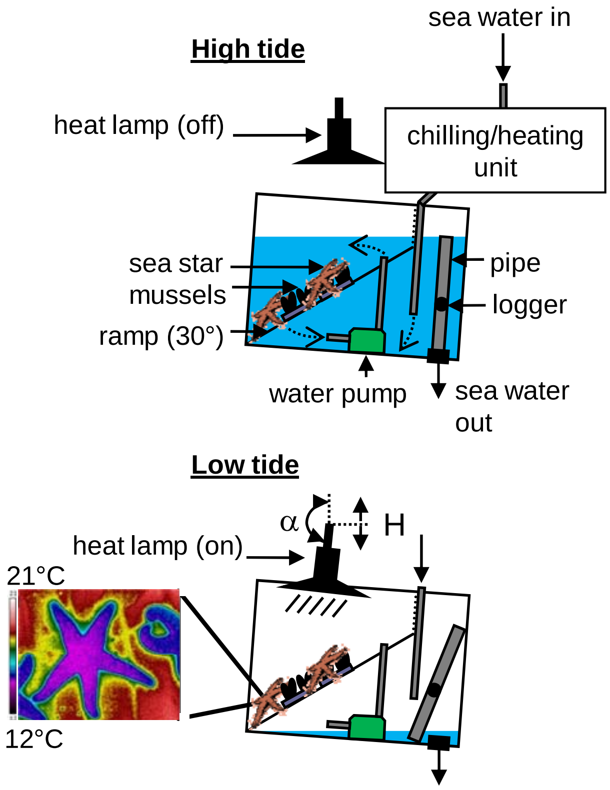

Figure S2. Design of the experimental setup used to simulate tide cycles and to control for body temperature of sea stars when immersed (BT_i) and emersed (BT_e). During high tide, chiller/heater units were used to control BT_i while a submerged pump circulated the sea water within the aquarium. Heat lamps were turned off during high tide periods. During low tide, sea water circulated continuously in the bottom of the aquarium to ensure a moderate and constant relative humidity. The inclined ramp prevented contact between animals and sea water. During low tide, the inclination (α) and the height (H) of the heat lamps were adjusted to control BT_e which was measured from the top of aquaria using an infrared camera (ThermaCAM 695, FLIR Systems, Boston, MA).

Appendix S3. Testing the potential effects on feeding rates of starvation/satiation and thermal history of mussels

We investigated potential alternative hypothesis to explain the variations in *Pisaster ochraceus* feeding rates observed in Experiments 1 and 2: the effects of starvation and satiation, as well as prey thermal history, on sea star feeding behavior.

Effect of starvation or satiation on sea star feeding

We investigated the potential effect of starvation and satiation on the sea star feeding dynamics in Experiments 1 and 2. Starvation could potentially have affected our results because sea stars were kept in the aquaria without food for 7 days prior to Experiments 1 and 2 (see main text). Therefore, there was concern that sea stars might be more motivated to feed on mussels at the beginning of the Experiments. Satiation effect, in contrast to starvation, may have altered the feeding behavior of sea stars towards the end of experimental periods because they were fed ad libitum. We tested whether either of these two effects occurred in our experiments. This was especially critical for the analysis of the results in the Experiment 2 with fluctuating conditions. Below we show that there was no bias toward (i) increased feeding response at the beginning of experimental periods, or (ii) decreased feeding response by the end of experimental periods.

We analyzed the feeding dynamics in Experiment 1, under constant conditions, and more particularly in the treatment with optimal thermal conditions, i.e. BT_i 13°C and BT_e 16°C. This set of conditions eliminates any effect of thermal stress. Therefore, animals in this treatment were likely most susceptible to effects of starvation and/or satiation. A linear regression model analysis indicated that the dynamics were strongly linear in time for each of the three replicate aquaria (Replicate 1: $y = 20.74\ x$, $R^2 = 0.96$, $P < 0.0001$; Replicate 2: $y =$

19.25 x, $R^2 = 0.98$, $P < 0.0001$; Replicate 3: y = 22.01 x, $R^2 = 0.97$, $P < 0.0001$) (Fig. S3A). The analysis of the residuals from these linear regression models showed that observation data points were all included within the 95% confidence prediction intervals (Fig. S3B, C, D). We concluded that our experimental approach did not cause any bias toward higher feeding rate due to starvation at the beginning of experimental periods or toward lower feeding due to satiation by the end of experimental periods. Therefore, the effects described in our study are all related to temperature treatments.

Several explanations can be provided to explain – and support – the choice of a 7-day acclimation period without food prior to experiments. *Pisaster ochraceus* can tolerate long periods of starvation. Wet body weight of the individuals does not change significantly during a 7-day period without food (Pincebourde *et al.* 2009), presumably due to this sea star's relatively low metabolism. Moreover, we collected the animals in July, when the sea stars had already eaten a lot throughout spring. This ensured that experimental individuals were not suffering nutritional stress.

Any effect of satiation is very unlikely during experimental periods as short as 20 days. Indeed, Sanford (2002) showed that feeding rate does not vary before 42 days in constant water temperature conditions in *P. ochraceus*. In that study, the sea stars were also submerged continuously (Sanford 2002). In another study with sea stars experiencing tide cycles in aquaria, no satiation effect was detected by the end of the 16-days experimental period (Pincebourde *et al.* 2008). Therefore, *P. ochraceus* is not satiated before > 20 days when fed ad libitum with its preferred prey (mussels) under conditions such as those imposed during our experiments.

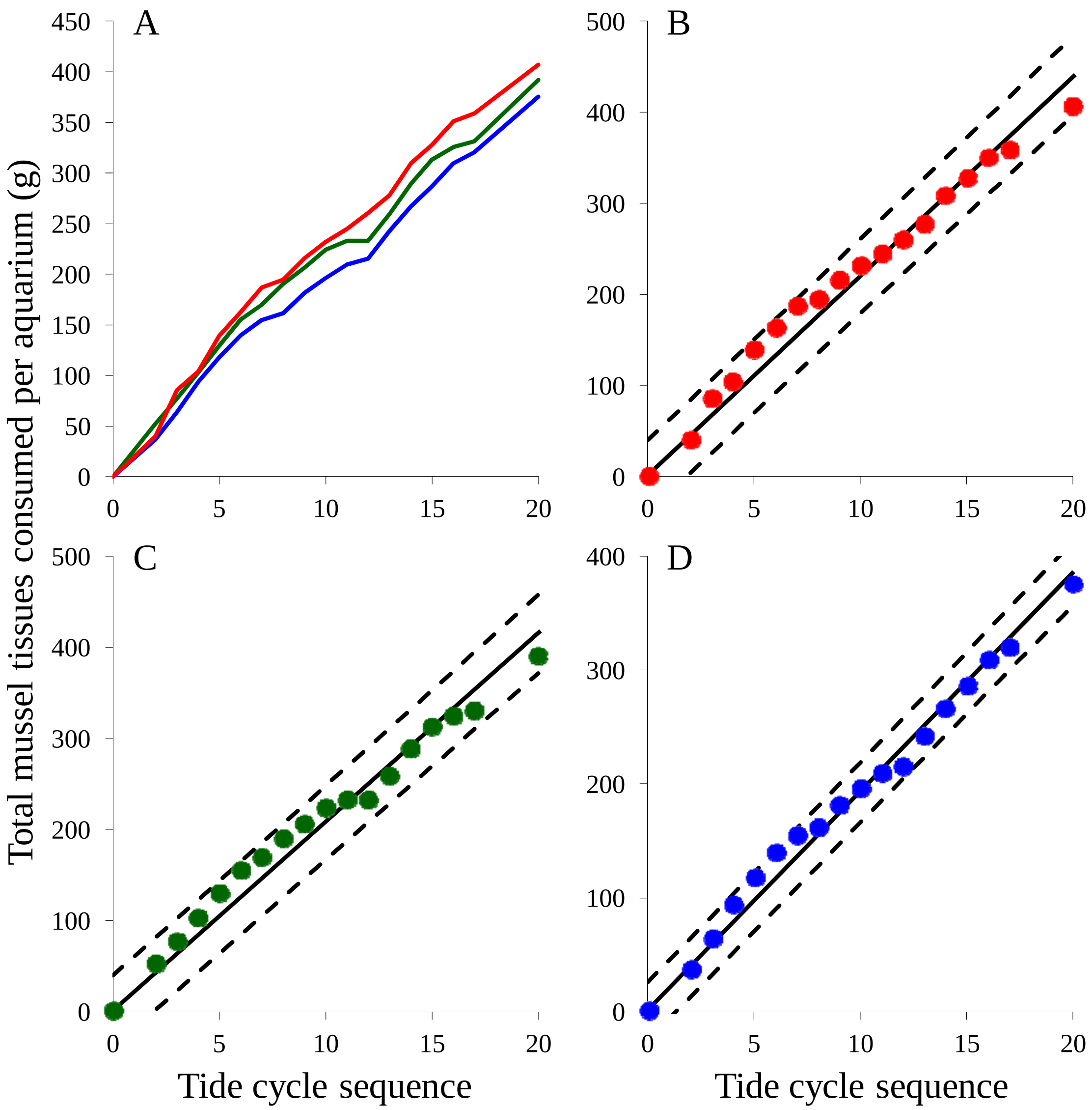

Figure S3. Temporal dynamics of mean mussel tissues consumed (cumulative) per aquarium (n = 3 replicates) during the 20-day period of Experiment 1 (constant conditions) in the treatment showing the most optimal thermal conditions (BT_i = 13°C; BT_e = 16°C). (A) Each curve represents a different replicate of this specific treatment. (B, C, D) Plots of the linear regression model (lines) on observations (data points) with the 95% confidence prediction interval (dotted lines for higher and lower bounds of the interval) for each replicate.

Effect of mussel thermal history on sea star feeding

In our experiments, heat lamps were used to manipulate sea star body temperature during low tide. Because the body temperature of mussels was also affected with this method, we tested the hypothesis that sea stars altered their predation rate in response to the thermal history of the mussels. Body temperature of mussels was the only fluctuating parameter in this additional 8-day experiment. A short stand pipe (height 14 cm) was used to set a low tide water level such that mussels were exposed to air (higher on the inclined ramp) whereas the lower portion of the ramp remained submerged. Because sea stars preferred to be submerged, they could retrieve mussels from the upper portion of the ramp during simulated high tide and feed on them on the lower portion of the tank. Thus, sea stars were continuously submerged in this experiment, as opposed to feeding trials where sea stars were forced to remain aerially exposed along with their prey (as would occur in the field). Four mussel aerial body temperature treatments (three replicate aquaria per treatment, four sea stars per aquarium) were applied (mean ± SD): 13.3 ± 0.7°C, 24.6 ± 1.6°C, 29.8 ± 2.3°C, and 34.9 ± 2.3°C, respectively. These mussel body temperatures were observed in the treatments used in Experiments 1 and 2. Mussel body temperatures were controlled using the same method described for sea stars. Mean water temperature (± SD) during the 8-day experiment was 13.1 ± 0.5°C. No effect of mussel body temperature on *P. ochraceus* feeding rate was detected (ANOVA, mussel temperature treatment as main factor: $F_{3,8} = 0.22$; $P = 0.88$). For example, the mean per capita feeding rate was 22.74 ± 1.26 g and 22.66 ± 0.88 g in the treatment with a mean mussel body temperature 13.3 ± 0.7°C vs 34.9 ± 2.3°C, respectively. Therefore, feeding rates were quite similar regardless of mussel temperature within an 8-day period. In our 20-day experiments (see main text – Experiments 1 and 2) fresh mussels were added into the all aquaria at day 10. We concluded that thermal history of the prey did not alter the feeding responses to temperature that we measured in Experiments 1 and 2.

REFERENCES

Pincebourde, S., Sanford, E. & Helmuth, B. (2008). Body temperature during low tide alters the feeding performance of a top intertidal predator. *Limnol. Oceanogr.*, 53, 1562-1573.

Pincebourde, S., Sanford, E. & Helmuth, B. (2009). An intertidal sea star adjusts thermal inertia to avoid extreme body temperatures. *Am. Nat.*, 174, 890-897.

Sanford, E. (2002). The feeding, growth, and energetics of two rocky intertidal predators (*Pisaster ochraceus* and *Nucella canaliculata*) under water temperatures simulating episodic upwelling. *J. Exp. Mar. Biol. Ecol.*, 273, 199-218.

Appendix S4. Relationship between sea star body surface temperature and internal body temperature.

Sea star body temperatures at low tide, when exposed to aerial conditions, were measured using an infrared imaging camera (ThermaCAM 695, FLIR Systems, Boston, MA) in our Experiments 1 and 2 (see main text). Infrared cameras offer the opportunity to measure body temperature patterns without disturbing the animals, which was especially critical in the case of the sea star *Pisaster ochraceus*. However, the infrared camera measures the temperature of body surface. In large ectotherms such as turtles, the internal body temperature can differ significantly from body surface temperature by several degrees (e.g. Dubois *et al.* 2009). Although the sear star *P. ochraceus* is a relatively small ectotherm, it has nevertheless a significant thermal inertia (Pincebourde *et al.* 2009). Therefore, there was concern that body surface and internal body temperature might be uncorrelated in *P. ochraceus*. Here, we tested whether body surface temperature was correlated to internal body temperature of sea stars. Individuals (n = 10) were put in the aquaria (one individual per aquarium) equipped with the heat lamps as described in Fig. S2. The position of heat lamps differed among aquaria to obtain a large range of thermal conditions. After 3 hours of exposure to aerial low tide conditions, we measured simultaneously body surface temperature via the infrared imaging camera and the internal body temperature. For the latter, we inserted a fine thermocouple 1 cm deep into the madreporite of the sea stars. This madreporite is located on the dorsal side. The two temperatures were correlated within the temperature range 15°C-27°C (Pearson correlation coefficient = 0.99, $P < 0.001$; linear regression model: $y = 1.1069\,x – 1.926$, $r^2 = 0.99$) (Fig. S4). Overall, body surface temperature in the central disc was an accurate predictor of internal body temperature in this species (RMSE = 0.58°C from the 1:1 line). There was a tendency for body surface temperature to be slightly higher by 1 to 2°C than internal body temperature at temperatures > 24°C. Amazingly, this deviation is comparable to the averaged temperature difference (~1.6°C) between carapace surface and internal body in a turtle of similar size and mass than *P. ochraceus* (Dubois *et al.* 2009).

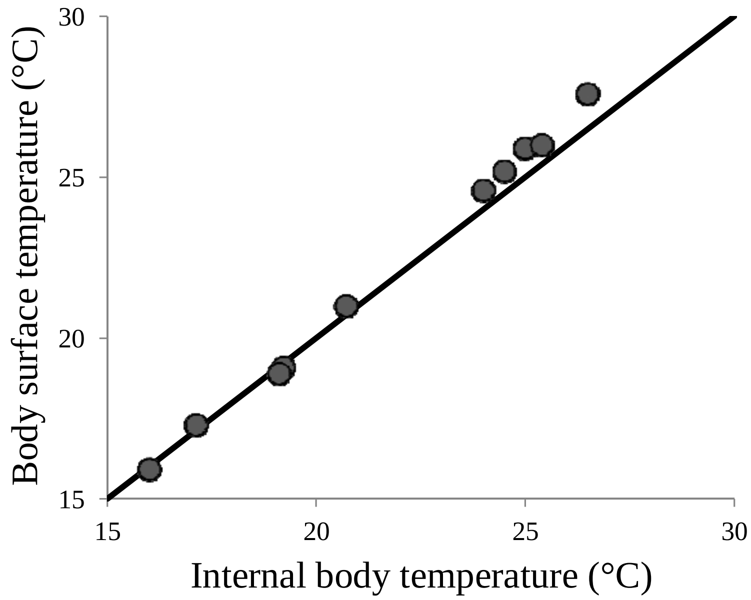

Figure S4. Body surface temperature, measured via the infrared imaging camera, as function of the internal body temperature, measured with a fine thermocouple. The line indicates the equality between the two temperatures.

REFERENCES

Dubois, Y., Blouin-Demers, G., Shipley, B. & Thomas, D. (2009). Thermoregulation and habitat selection in wood turtles *Glyptemys insculpta*: chasing the sun slowly. J. Anim. Ecol., 78, 1023-1032.

Pincebourde, S., Sanford, E. & Helmuth, B. (2009). An intertidal sea star adjusts thermal inertia to avoid extreme body temperatures. *Am. Nat.*, 174, 890-897.

Appendix S5. Temporal series of body temperatures in the field

Field temperature recordings showed that a wide range of BT_i-BT_e combinations is possible although a slight correlation existed in the low intertidal zone at the wave-protected site (see Fig. 3 in main text). Another way of illustrating this independency between these two variables is to show the temporal series of mean daily maximal body temperatures during low and high tides at our study sites (Fig. S5a). A similarly broad range of BT_i-BT_e combinations was apparent at intertidal sites located 700 km to the north in Oregon (Fig. S5b; Sanford 2002), suggesting that this is probably a general pattern of coastal upwelling systems. At the beginning of a low tide, the BT_e of organisms equals BT_i. This correlation exists therefore only if there is not enough time for terrestrial conditions to alter BT_e due to either very short emersion time (such as in the low intertidal at the wave-protected site) or frequent wave splash (such as at the wave-exposed site). The lack of correlation in the low intertidal zone at the wave-exposed site results probably from the variation in wave splash intensity on subsequent days. The weak correlation in the high intertidal zone at the wave-exposed site might be due to effect of local topography. Indeed, large pools appeared in the high intertidal, frequently re-filled with fresh sea water via wave-splash. The loggers located nearby may have been influenced by this phenomenon. Such physical links between BT_i and BT_e were suggested in mussels (Gilman *et al.* 2006). In *Pisaster ochraceus,* BT_i and BT_e are also linked through a novel thermoregulatory strategy consisting of adjusting the sea star thermal inertia at low tide (Pincebourde *et al.* 2009). Physical and physiological interactions between BT_i and BT_e are likely to be widespread among intertidal organisms.

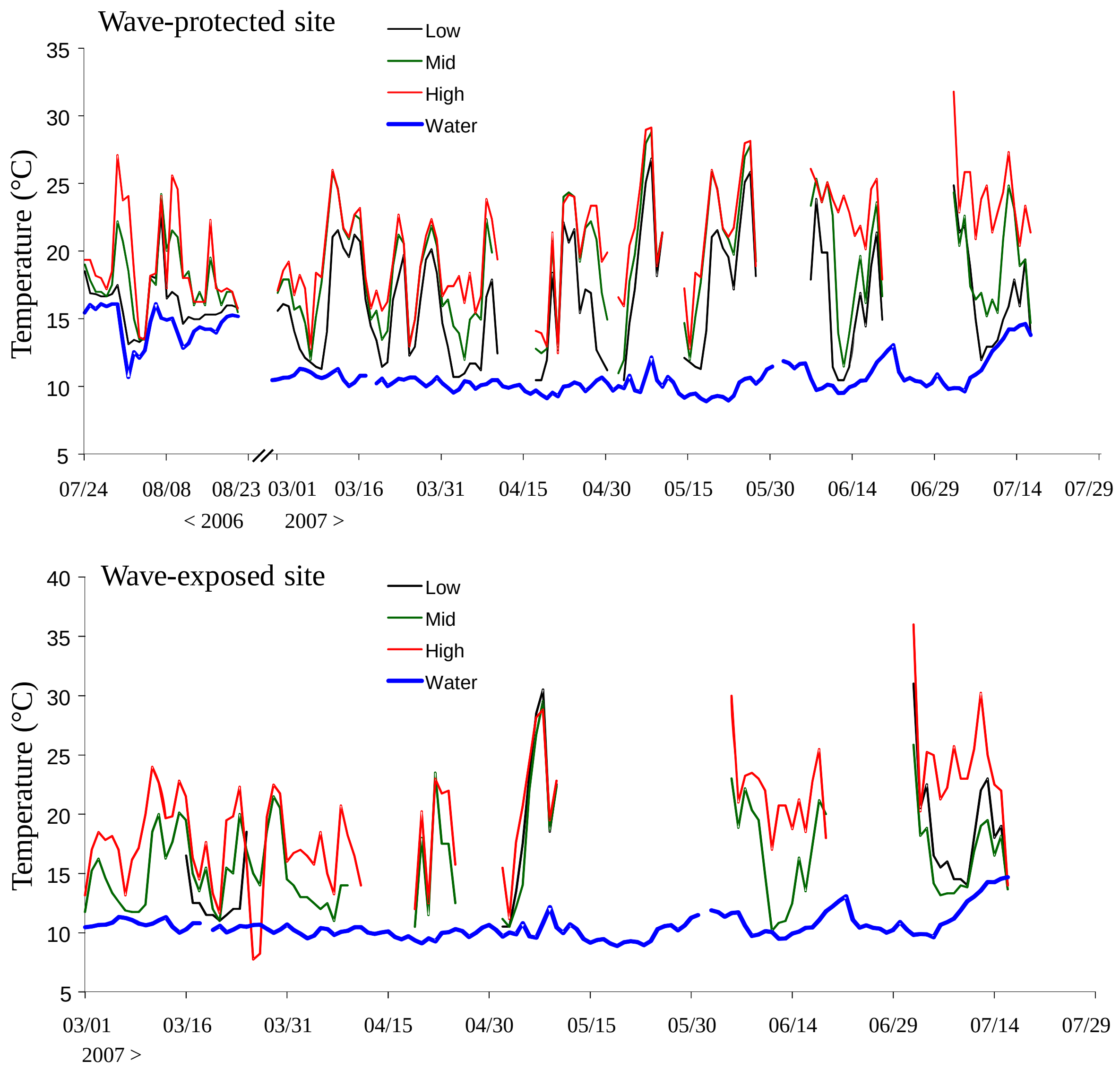

Figure S5a. Temporal patterns in sea star body temperature at the wave-protected (2006 and 2007) and wave-exposed (2007) sites in the Bodega Marine Reserve (Bodega Bay, California). Mean daily maximal temperature is shown for dataloggers in the low (black), mid- (green) and high intertidal zone (red). The intertidal position of dataloggers is given in Fig S1. The blue curve indicates the mean daily water temperature as a proxy for underwater sea star body temperature. Interruptions along the curves were caused by the loss of the dataloggers from wave disturbance.

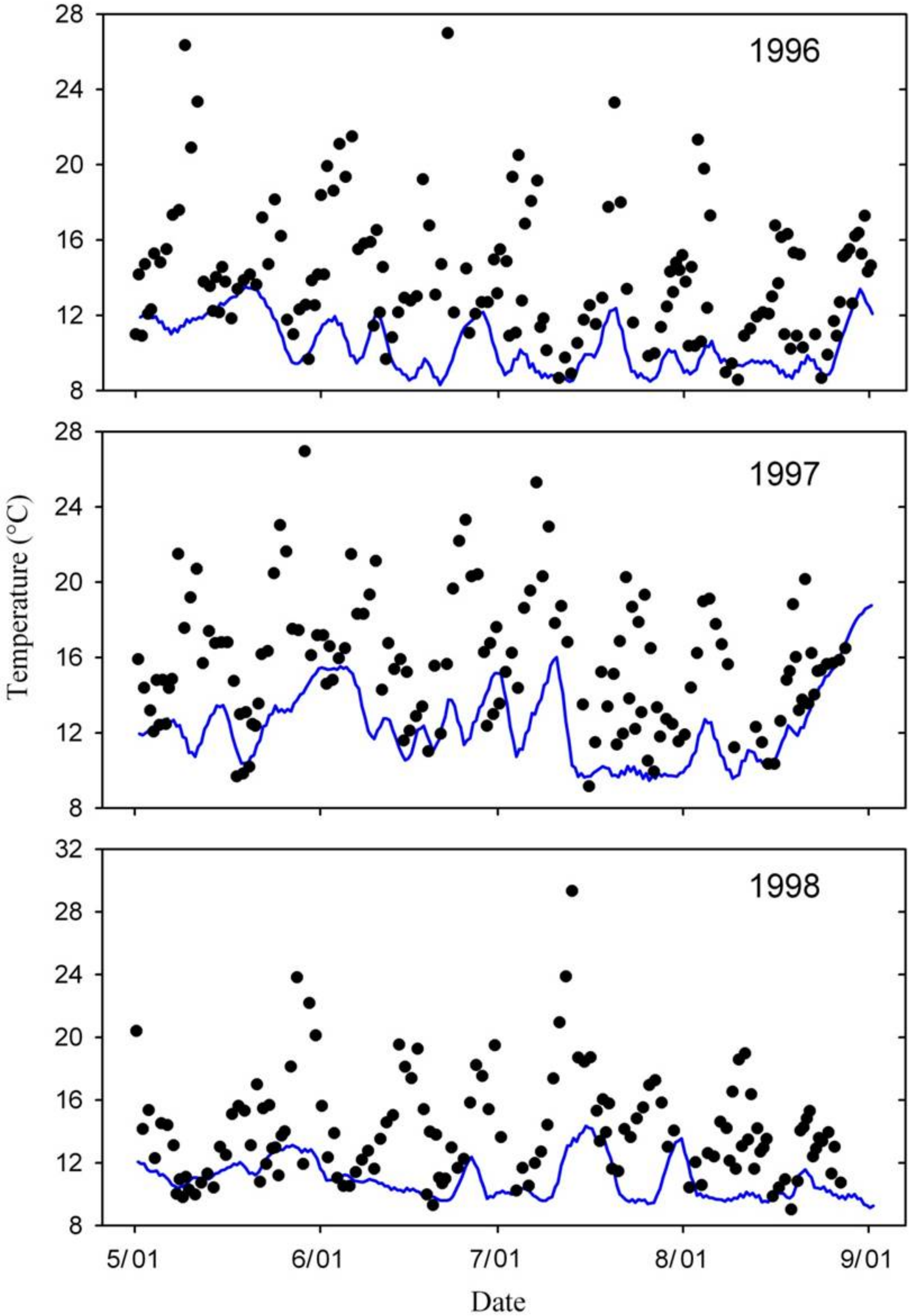

Figure S5b. Temporal patterns in sea star body temperature at Neptune State Park on the central Oregon coast during summers (1996-1998). Blue line indicates water temperature at high tide (a proxy for BT_i), smoothed with a running means function (see Sanford 2002). Data points are emersed body temperature (BT_e) in the low intertidal zone during each low tide period of emersion, estimated from data loggers deployed at three wave-exposed locations at 0.7 m above MLLW (see Sanford 2002 for additional details).

REFERENCES

Gilman, S.E., Wethey, D.S. & Helmuth, B. (2006). Variation in the sensitivity of organismal body temperature to climate change over local and geographic scales. *Proc. Natl. Acad. Sc. USA*, 103, 9560-9565.

Pincebourde, S., Sanford, E. & Helmuth, B. (2009). An intertidal sea star adjusts thermal inertia to avoid extreme body temperatures. *Am. Nat.*, 174, 890-897.

Sanford, E. (2002). The feeding, growth, and energetics of two rocky intertidal predators (*Pisaster ochraceus* and *Nucella canaliculata*) under water temperatures simulating episodic upwelling. *J. Exp. Mar. Biol. Ecol.*, 273, 199-218.

Appendix S6. A 2D graphical view of feeding rates under constant conditions (Experiment 1)

A conventional 2D graphical representation of the results shown in Fig. 4 (Experiment 1) is provided here. This alternative, in particular, facilitates plotting the standard deviation of the aerial body temperatures at low tide. The total feeding rate (over the 20-day period) is provided to complement the data shown in the core of the article.

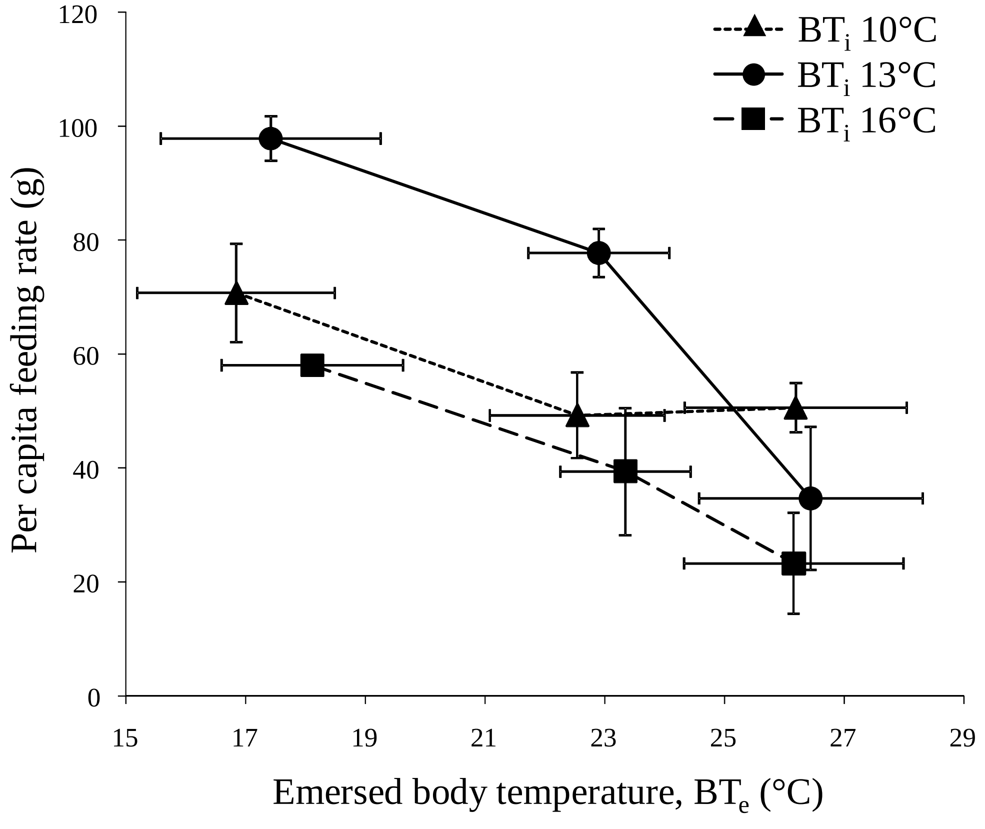

Figure S6. Per capita feeding rate (total over the 20-day experimental period; mean ± SD) as a function of emersed body temperature (mean ± SD) at low tide treatments in Experiment 1 for the different immersed body temperature conditions.

Appendix S7. Table S1: Compound statistics of the 9 treatments in the Experiment 2

Table S1. Compound average and variance in the 9 treatments of the fluctuating Experiment 2. Both mean and variance were calculated from the hourly temperature series including aquatic and aerial temperatures. The comparisons made in the main text are indicated by the groups A, B and C.

Treatments*	**Overall mean (°C)**	**Overall variance**	**Groups to be compared**
BT_e-Constant x BT_i-Constant	15.01	8.04	
BT_e-Constant x BT_i-Down	14.99	13.58	A
BT_e-Constant x BT_i-Up	14.68	14.03	A
BT_e-Chronic x BT_i-Constant	15.00	10.03	B
BT_e-Acute x BT_i-Constant	15.00	10.12	B
BT_e-Chronic x BT_i-Down	14.98	15.99	C
BT_e-Chronic x BT_i-Up	14.67	15.61	C
BT_e-Acute x BT_i-Down	14.97	15.78	C
BT_e-Acute x BT_i-Up	14.66	16.00	C

* Refer to Fig. 2 in main text for legend of conditions and treatments.